Adsorption of Methane and Hydrogen on Mesocarbon Microbeads by Experiment and Molecular Simulation

Xiaohong Shao and Wenchuan Wang*

Lab of Molecular and Materials Simulation, College of Chemical Engineering, Beijing University of Chemical Technology, Beijing 100029, China

Ruisheng Xue and Zengmin Shen

National Carbon Fiber Center, College of Materials Engineering, Beijing University of Chemical Technology, Beijing 100029, China

Received: June 17, 2003; In Final Form: January 9, 2004

The activated mesocarbon microbeads (a-MCMBs) with high BET specific surface area of 3180m^2/g are prepared. Experimental characterization of a-MCMBs is carried out in terms of the adsorption isotherm of nitrogen at 77 K by the ASAP-2010 apparatus. Then, methane and hydrogen adsorption isotherms on a-MCMBs are measured by the IGA-003 gravimetric analyzer at 298 K and 77 K. The pores of a-MCMBs are described as slit-shaped with a pore size distribution (PSD). The PSD is determined by a combined method of grand canonical Monte Carlo (GCMC) simulation and statistics integral equation (SIE) from the experimental isotherm of nitrogen on a-MCMBs. In GCMC simulation, methane and hydrogen molecules are modeled as the Lennard-Jones spherical molecules, and the well-known Steele's 10-4-3 potential is used to represent the interaction between the fluid molecule and the solid wall. Good agreement between simulated and experimental data indicates that our model represents well the mechanism of adsorption on a-MCMBs. Then, this model is used to predict adsorption of methane and hydrogen over a wide range of pressure up to 12 MPa. The prediction shows that adsorption amount of methane reaches 36 wt % at 298 K and 4 MPa, which is superior to the results in the literature. The hydrogen adsorption amount at 10 MPa can reach 3.2 wt % and 15 wt % at 298 K and 77 K, respectively, which are also higher scores, compared with the other carbon materials.

Introduction

Natural gas and hydrogen are the green energy that can be stored by adsorption in carbonaceous adsorbents.[1−5] A major problem of adsorption storage of natural gas and hydrogen is to choose appropriate adsorbents. Interestingly, diversified experimental results of hydrogen adsorption on carbonaceous porous materials are reported in the literature. For example, Wang et al.[5] report that hydrogen adsorption on the single-walled nanotubes (SWNT) is 2 wt %, while the result of Darkrim et al.[6] reaches 11 wt % at 10 MPa and 80 K. As for the adsorption uptakes at ambient temperature, Liu et al.[7] found that the adsorption of hydrogen on SWNT can reach 4.2 wt % at 300 K and 12 MPa. In contrast, the CEA laboratory of France[8] reports that the adsorption is only 0.2 wt % at 300 K and 10 MPa on SWNTs. Several articles[8,9−12] have delivered comprehensive reviews on experimental and theoretical work on hydrogen adsorption on activated carbons, single-walled nanotubes (SWNT), multiwalled nanotubes, and graphite nano-fibers (GNF). Among theoretical researches, using molecular simulation, Wang and Johnson[9−11] demonstrated that it is impossible to get a high storage amount even by taking into account the physisorption and chemisorption on carbonaceous porous materials. It is most likely that the hydrogen storage in the materials is still an argumentative topic.

Natural gas has a considerable advantage over conventional fuels from the environmental point of view.[13] Adsorbed natural gas (ANG) is a more economical and safer solution than the conventional method of compressed natural gas (CNG). Many researchers reported their results on adsorption storage of natural gas, and focused on its major component methane, in particular.[13−16] Lozano-Castello et al.[15] carried out a detailed review on methane storage in different porous carbonaceous materials. They found that the adsorption of methane can reach 14.8 wt % on activated carbon fibers at 298 K and 4 MPa. The uptakes could reach as high as 19.1 wt % at 298 K and 4MPa on a powdered activated carbon, which is higher than those on activated carbon fibers (ACFs). In summary, despite many results reported, it is still a challenging task to prepare and test promising carbonaceous adsorbents for adsorption storage of methane and hydrogen.

As a new type of porous materials, mesocarbon microbeads (MCMBs) are micro carbon spheres produced by mesophase pitches,[17] which have been mainly used as filler in paints, elastomers, and plastics to modify the mechanical, electrical properties of the materials.[17,18] Particularly, MCMBs are widely used in the lithium-ion batteries[19] recently. After activating, the activated MCMBs (a-MCMBs) with high specific surface area greater than 2630 $m^2\ g^{-1}$ can be prepared, which is called a super high surface area carbon or super surface carbon.[17] Many investigations[17,18,20,21] show that a-MCMBs are expected to be more ordered in structure than the activated carbon fibers (ACF). In addition to experimental researches, Thomson and Gubbins[21] characterized a-MCMB samples with the nitrogen isotherm to test their Reverse Monte Carlo model. However, little was

* Corresponding author. Fax +86-10-64427616. E-mail: wchwang@163bj.com.

10.1021/jp035715d CCC: $27.50
Published on Web 02/06/2004

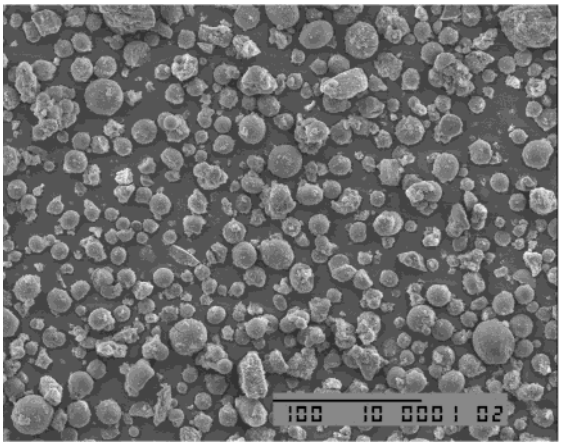

Figure 1. The SEM photo of MCMBs at the voltage of 19 kV, taken from the literature.[22]

reported to use a-MCMBs to store energy, though the a-MCMBs could be a good adsorbent for storage of natural gas and hydrogen.

In this work, we use a sample of a-MCMBs prepared by our group for adsorption storage of hydrogen and methane by experiment and computer simulation. Experimental characterization is conducted in terms of the isotherm of N_2 at 77 K. Then, the adsorption isotherms of hydrogen and methane are measured by the Intelligent Gravimetric Analyzer (IGA-003) up to 1.0 MPa at 298 and 77 K, respectively. To evaluate the adsorption storage capacities, a model for the a-MCMBs is developed. In this model, the pores of a-MCMBs are described as slitlike with a pore size distribution, which is determined by GCMC and a statistical integral equation. On the model proposed, we predict the capabilities of a-MCMBs for adsorption storage of methane and hydrogen by the GCMC method, respectively, covering a wide range of pressure at 77 and 298 K. Finally, the adsorption capabilities of the a-MCMBs are compared with other results reported in the literature.

Preparation of Sample a-MCMBs and Experimental Measurements

Sample Preparation. We first mixed the filtrated residue of petroleum and carbon black (2 wt %). Then, we maintained the mixture in an autoclave with a nitrogen environment at 680 K for 4.5 h. By using pyridine separating the resultant, raw carbon spheres were prepared. Then, the carbon spheres and KOH (the weight ratio is 1:8) were put into a furnace and surrounded by nitrogen for activated treatment. The resultant was heated to 1123 K for 1.0 h. Finally, the a-MCMB sample was obtained after cleaning and drying. Detailed information can be found in the literature.[22,23]

Scanning electron microscopy (SEM) images were obtained by means of the Cambridge S-250 MK III instrument, which was operated at 19 kV in the secondary electron imaging mode. The appearance of the MCMBs is shown in Figure 1.[22] Most of them are sphere-shaped and of diameters of 20 μm. After activating by KOH, the a-MCMBs were prepared and they take ellipse-like shapes sized from 10 to 20 μm, as is shown in Figure 2. Figure 3 gives a high-resolution SEM photo of a single bead, showing that there are some external pores on the bead. The external pores work as channels, where fluid molecules can pass through.

Experimental Measurement of an Adsorption Isotherm for Nitrogen at 77 K. The Accelerated Surface Area and Porosimetry Apparatus (ASAP 2010, Micromeritics Ins. Corp.)

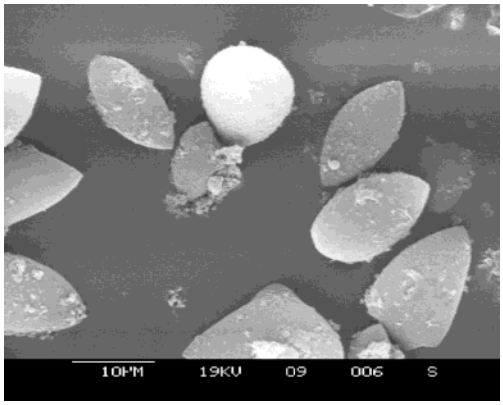

Figure 2. The SEM photo of a-MCMBs by SEM at the voltage of 19 kV.

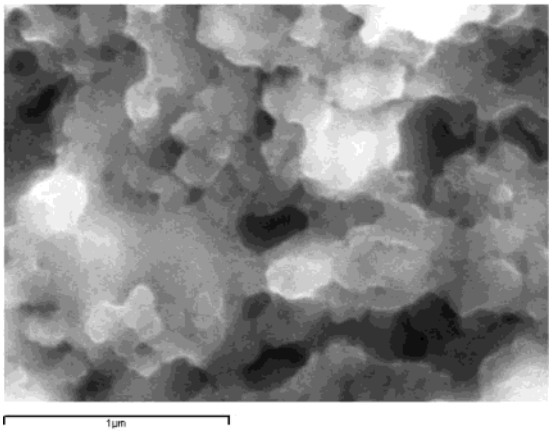

Figure 3. The SEM photo of a single bead of a-MCMBs.

was used to measure the nitrogen adsorption isotherm in the range of relative pressure, p/p_0, where p_0 is the saturated vapor pressure of the system, from 0.1 Pa to 0.1 MPa at 77 K. As is required, the sample was outgassed at 473 K for 15 h before the measurements.

IGA-003 Gravimetric Adsorption Measurements. The Intelligent Gravimetric Analyzer (IGA-003, Hiden) was used to measure the adsorption isotherms of methane and hydrogen for the sample a-MCMBs by using the gravimetric method. In IGA-003, an ultra-sensitive microbalance of resolution 0.2 μg is mounted in the thermostated heatsink with high precision temperature control. The sample weighed about 100 mg for each run. Before the measurements, the sample in the vessel of IGA-003 was vacuumed up to 10^{-5} Pa and outgassed at 573 K for 15 h. The measurements were carried out at 77 and 298 K in terms of the built-in water and liquid nitrogen baths, respectively. The highest adsorption pressure was 1.0 MPa for the sensor limitation of IGA-003. To guarantee equilibration, 1.5 h was needed for a data point in the measurements at 77 K, while only 0.5 h for a data point at 298 K.

Methane used in experiments is of the purity of 0.999 (mol), produced by Bright Gas Factory, Dalian, China. To guarantee the quality of measurements for hydrogen particularly, the purity of hydrogen is 0.99999 (mol), produced by the Oxygen Company of Fu Shun, China.

Modeling of Adsorption on a-MCMBs and Grand Canonical Monte Carlo Simulation. A model of adsorption on a-MCMBs relies on the description of the mechanism and characteristics for a-MCMBs, and interactions between the fluid−fluid and fluid−adsorbent of interest on molecular level. More importantly, understanding of the molecular mechanism of

TABLE 1: Parameters of Potential Models for Fluids and a-MCMBs[a]

N_2		H_2		CH_4		solid wall of a-MCMB	
σ/nm	$\epsilon \cdot k^{-1}$/K	σ/nm	$\epsilon \cdot k^{-1}$/K	σ/nm	$\epsilon \cdot k^{-1}$/K	σ/nm	$\epsilon \cdot k^{-1}$/K
0.375	95.2	0.296	34.2	0.381	148.1	0.34	28.0

[a] The parameters for N_2, H_2, CH_4, and the solid wall of a-MCMBs are taken from refs 21, 27, and 31, respectively.

adsorption provides a basis for computer simulation, which is a useful tool for prediction of the performance of the adsorbent a-MCMBs.

Modeling of a-MCMBs. Honda[24] proposed a structural model of MCMBs. In the model, a bead is formed by slit-shaped carbon layers. The distance between two layers is the lattice distance, which is equal to 0.335 nm. Therefore, many researchers account for a-MCMBs more ordered in structure than ACFs. In addition, Thomson and Gubbins[21] characterized a-MCMB samples as slit-shaped pores and used the nitrogen isotherm of a-MCMBs in their Reverse Monte Carlo simulation.

It is noticed that after activating by KOH, heterogeneity of the pores of a-MCMBs becomes pronounced, and should therefore be taken into account in characterization. Consequently, the a-MCMBs are modeled as a porous material possessing slit pores with a pore size distribution (PSD) in this work.

Fluid−Fluid Molecular Interactions. In GCMC simulation, methane and hydrogen molecules are considered as the Lennard-Jones(LJ) spherical molecules. The fluid−fluid interactions are described by the cut and shifted Lennard-Jones potential,

$$\phi_{ff} = \begin{cases} \phi_{LJ}(r) - \phi_{LJ}(r_c) & r < r_c \\ 0 & r > r_c \end{cases} \quad (1)$$

where r is the intermolecular distance, r_c is the cutoff radius, $r_c = 5\sigma_{ff}$, ϕ_{LJ} is the full LJ potential, given by

$$\phi_{LJ}(r) = 4\epsilon_{ff}\left[\left(\frac{\sigma_{ff}}{r}\right)^{12} - \left(\frac{\sigma_{ff}}{r}\right)^{6}\right] \quad (2)$$

where ϵ_{ff} and σ_{ff} are the energy and size parameters of the fluid, respectively.

Obviously, methane is a typical LJ spherical molecule in nature. However, the quantum effect of hydrogen molecules on adsorption simulation is still a topic under discussion. Wang et al.[25] discussed the quantum effect of hydrogen molecules systematically. They evaluated the Silvera and Goldman's (SG) potential[26] that accounts for the quantum effect, and three LJ hydrogen potentials proposed by Buch,[27] Buck et al.,[28] and Dondi and Valbusa[29] from simulations and experiment over a wide range of temperature and pressure. It is found that the hydrogen internal energies exhibit deviations with and without accounting the quantum effect. But the Buch's parameters[27] gave densities that agree with experiment almost as well as the results from the SG potential, except that the temperature is below 30 K. Consequently, the LJ potential and Buch's parameters were adopted to simulate the hydrogen adsorption on a-MCMBs in this work, as is shown in Table 1.

Fluid−Wall Molecular Interactions. The pores of a-MCMBs can be described as slit-shaped with a pore size distribution. Therefore, the interaction between a solid wall and a fluid molecule is given by the well-known Steele's 10-4-3 potential[30]

$$\phi_{fw}(z) = 2\pi\rho_w\epsilon_{fw}\sigma_{fw}^2\Delta\left[0.4\left(\frac{\sigma_{fw}}{z}\right)^{10} - \left(\frac{\sigma_{fw}}{z}\right)^{4} - \left(\frac{\sigma_{fw}^4}{3\Delta(0.61\Delta + z)^3}\right)\right] \quad (3)$$

where ρ_w is the number density of the solid wall, $\rho_w = 114$ nm^{-3}, and the subscript w represents the wall, Δ is the distance between lattice planes, and is set to 0.335 nm, z is the normal distance between a fluid molecule and one of the solid walls, ϵ_{fw} and σ_{fw} are the cross interaction parameters, which are obtained from the Lorentz−Berthelot combing rules. The parameters of fluid−fluid and fluid−solid used in this work are given in Table 1.

Grand Canonical Monte Carlo Simulation. By using the grand canonical Monte Carlo (GCMC) method, where the chemical potential, the volume, and the temperature are the independent variables, adsorption of methane and hydrogen on a-MCMBs was simulated. In our simulation, the periodic boundary conditions were imposed only in the x and y directions. All the variables were reduced with respect to the fluid molecules. The initial configuration was generated randomly. For a fixed cell, three types of moves were used to generate a Markov chain, including moving, creating, and deleting a molecule. The three types of moves have the same probability and each has different receiving opportunities. For every state, we generated 2×10^7 configurations and discarded the first 1×10^7 configurations to ensure the equilibration. During the simulation, the average number of fluid molecules could reach about 1000. Details for the GCMC method can be referred to our previous work.[2,3,32,33]

Results and Discussion

Characterization of a-MCMBs by the Adsorption Isotherm of N_2 at 77 K. The sample of a-MCMBs was characterized by using the ASAP-2010 adsorption apparatus. The isotherm of N_2 at 77 K is shown in Figure 4. The BET specific surface area, pore volume and average pore size of the sample obtained from ASAP-2010 are given in Table 2.

The results indicate that our sample has a high BET specific surface area, S_{BET}, 3180m^2 g^{-1}. In addition, the average pore size H_{av} is 2.47 nm. According to the IUPAC classifications of pores, the sample resides in the range of mesoporous materials. Impressively, among all the articles published about a-MCMBs,[17,18,34,35] the specific surface area of our material seems to be higher than the others.

Determination of the Pore Size Distribution by GCMC and Statistical Integral Method. For any real porous materials, the pore size heterogeneity always exists. As is mentioned above, the slit-shaped pores with PSD represent the real pore structure of our sample. Each pore size will contribute to the total adsorption isotherm in proportion to the fraction of the total volume of the sample. Adsorption in different size pores can be simulated by GCMC method. The simulation isotherm from a PSD is, thus, described as a combination of isotherms in individual slit pores using the statistics integral equation[36−38]

$$\Gamma_{sim} = \sum_{H_{min}}^{H_{max}} \Gamma(H)g(H)\Delta H \quad (4)$$

where Γ_{sim} is the adsorption calculated by the PSD, $\Gamma(H)$is the calculated adsorption amount in a single model pore of width

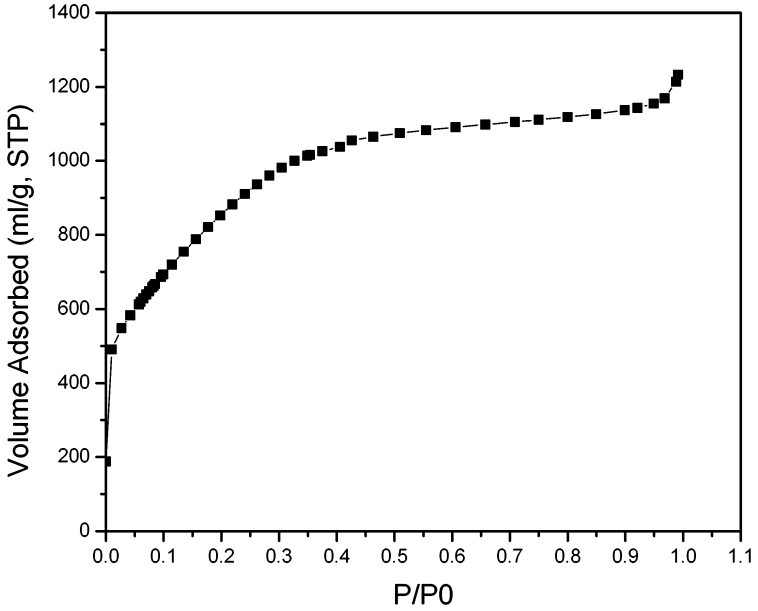

Figure 4. The isotherm of nitrogen at 77 K on a-MCMBs, measured by ASAP 2010.

TABLE 2: Properties for a-MCMBs Measured by ASAP-2010

BET specific surface area	pore volume	average pore size
$S_{BET}/(m^2\ g^{-1})$	$V_p/(cm^3\ g^{-1})$	H_{av}/nm
3180	1.9	2.47

H, and $g(H)$ is the PSD, which is defined as the fraction of the pore of width H occupying total pores in the a-MCMBs. H_{max} and H_{min} are minimum pore and maximum pore sizes in the case investigated, respectively. Accounting for the pore size range of our sample, H_{min} and H_{max} are set to 0.75 and 4.5 nm here, and ΔH is set to 0.375 nm. The PSD can be solved by minimizing the deviation between the experimental isotherm and the simulation results, L,[39]

$$L = \sum_{i=1}^{n} [\Gamma_{sim}(p_i/p_0) - Y(p_i/p_0)]^2 \qquad (5)$$

where Γ_{sim} is the adsorption simulated by GCMC, $Y(p_i/p_0)$ is the experimental data, n is the number of experimental data points.

It is interesting to look into the adsorption behavior of a constituent pore in the PSD. Figure 5 presents the isotherms by GCMC method for single pore size ranging from 0.75 nm to 4.5 nm. It is found that there exist three types of nitrogen isotherms in the pores. As is seen in Figure 5a, adsorption achieves easily the saturated densities at low pressures for the pores of 0.75 nm, 1.125 nm, and 1.5 nm, which belongs to type I isotherm for microporous materials on the IUPAC classification.[40] When the pore size is greater than a few times of the adsorbate molecule diameter, capillary condensation would occur. Here, for the pores from 1.875 to 3.375 nm, sudden vertical jumps in adsorption, which represent capillary condensation,[41] are observed, as is shown in Figure 5b. When the pore size is enlarged to 3.75−4.5 nm, the adsorption exhibits a monotonic increase with pressure for macropores (see Figure 5c). All the observations indicate that the adsorption taking place in our sample is, in fact, a combination of the uptakes of the three types of pores.

Corresponding to the adsorption isotherms in Figure 5, the PSD for the sample is obtained, shown in Figure 6. It is found in Figure 6 that the pores of widths ranging from 1.5 to 3.0 nm take up the main structure of our sample. Then, we plotted the simulation data obtained from the PSD along with the experimental isotherm in Figure 7. It is observed that all the simulated data coincide well with the experimental curve. For a comparison, the isotherm simulated from the average pore size, 2.47 nm, is also presented in Figure 7, in which there is a vertical jump representing capillary condensation for the single pore size. The large deviation between the isotherm simply from the average size and the experimental data suggests the introduction of the PSD is vital for characterization of the sample. Consequently, the PSD is used in our subsequent calculation and prediction of the adsorption behavior of the sample of a-MCMBs.

Experimental Adsorption Isotherms for Methane and Hydrogen at 298 and 77 K by IGA-003. The upper limit of the adsorption pressure for the gravimetric analyzer IGA-003 used in our experiment is 1.0 MPa, because of the limitation of the pressure transducer of the apparatus. Therefore, we measured the isotherms for methane and hydrogen up to 1.0 MPa at 298 and 77 K, respectively, which are presented in Figures 8−11. It is found from Figures 8 and 9 that the experimental isotherms for methane and hydrogen are almost linear at ambient temperature, 298 K. In addition, the methane adsorption can reach 14.73 wt %, while the hydrogen adsorption is only 0.3 wt % at the pressure of 0.99 MPa. Figure 10 shows the hydrogen adsorption at 77 K, which reaches a high uptake of 7.8 wt % at 0.95 MPa. As is expected for methane, when we measured carefully the adsorption and desorption isotherms at 77 K, capillary condensation and the hysteresis phenomenon were observed, which are shown in Figure 11.

Comparison of Experimental and Simulated Isotherms and Test of the Model Proposed. We first compare the experimental and simulated isotherms that were calculated by incorporating the PSD to test our model. As is seen in Figures 12−14, striking agreements between the experimental and simulated isotherms for hydrogen and methane indicate that our model is a good representation of the adsorption of methane and hydrogen on a-MCMBs. For a comparison, the simulated isotherms from the average pore size of 2.47 nm are also shown in Figures 12−14, where significant deviations from the experiment appear for the reasons explained above.

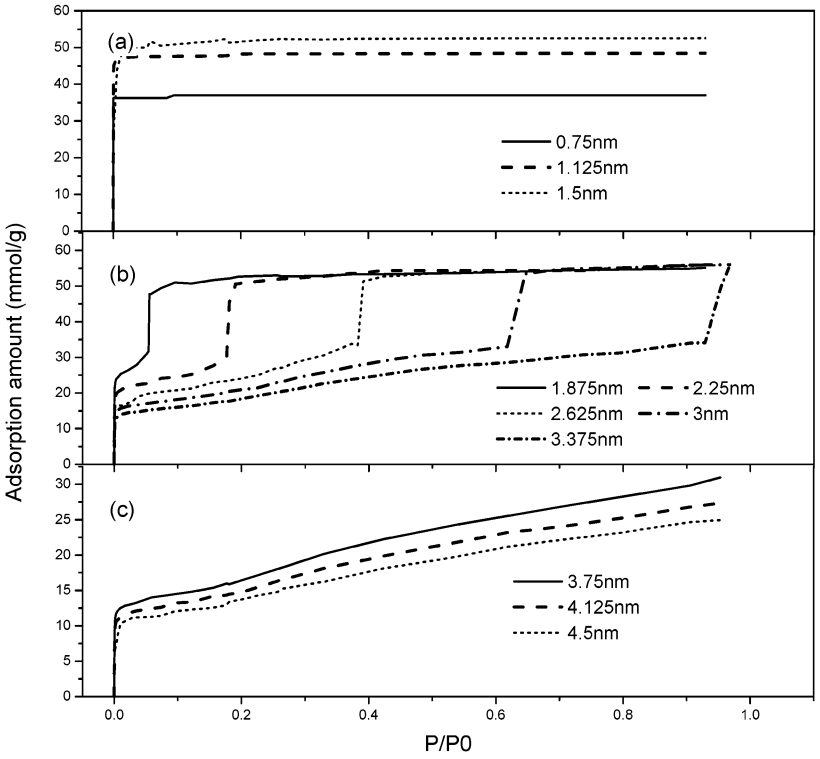

Figure 5. Adsorption isotherms of nitrogen in single pore ranging from $H = 0.75$ nm to $H = 4.5$ nm at 77 K, $\Delta H = 0.375$ nm. (a) The pore size: solid line ($H = 0.75$ nm), dash line ($H = 1.125$ nm), short dash line ($H = 1.5$ nm); (b) The pore size: solid line ($H = 1.875$ nm), dash line ($H = 2.25$ nm), short dash line ($H = 2.625$ nm), dash dot line ($H = 3$ nm), short dash dot line ($H = 3.375$ nm); (c) The pore size: solid line ($H = 3.75$ nm), dash line ($H = 4.125$ nm), short dash line ($H = 4.5$ nm).

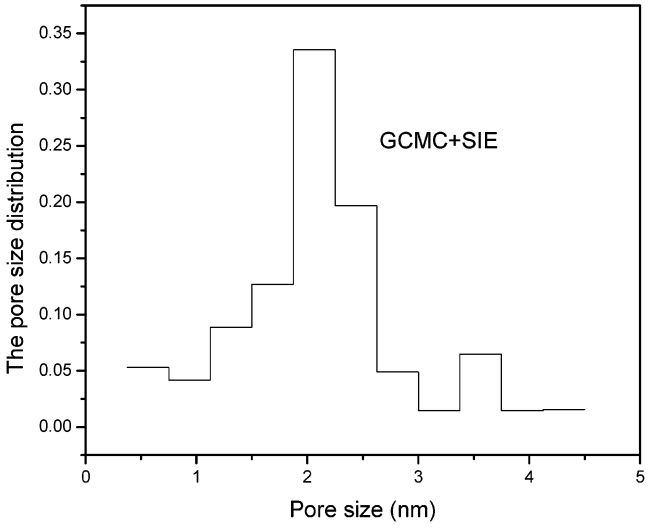

Figure 6. The pore size distribution of a-MCMB by GCMC and SIE.

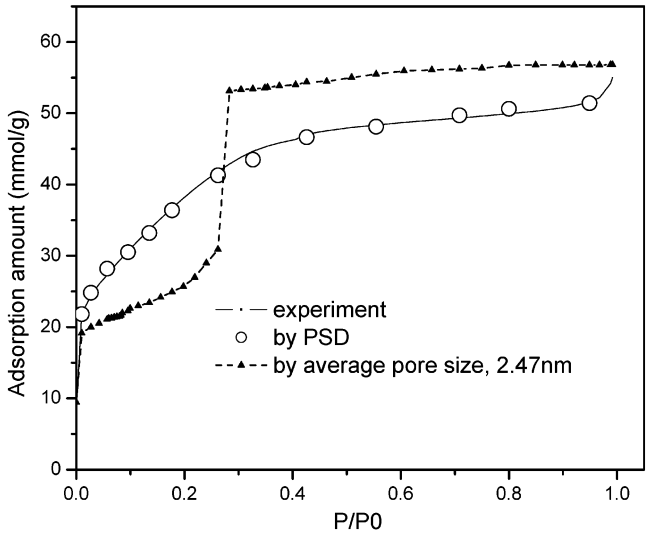

Figure 7. Comparison between experimental and simulation isotherms of nitrogen fitted by using PSD and the average pore size, at 77K (— · — experimental data, ○ by PSD, and —▲— by the average pore size, $H_{av} = 2.47$ nm).

From the discussion above, we find that the simulation agrees well with the experiment data by using GCMC with PSD. Consequently, the model proposed can be furthermore used for prediction of the adsorption on a-MCMBs in different conditions.

Prediction of Adsorption Isotherms for Methane and Hydrogen. GCMC and PSD were used to predict the adsorption amount of methane and hydrogen on a-MCMBs at higher pressures and at 298 K. It is found in Figure 15 that of a parabola-like curve, the uptake of methane increases with pressure drastically in the range of pressure from 0.5 to 2.5 MPa. The methane adsorption can reach 36 wt % at 4.0 MPa and 298 K. To our knowledge, this uptake is superior to those reported in the literature.[15] In contrast, hydrogen adsorption exhibits a linear increase with pressure, as is shown in Figure 16, because 298 K is a highly supercritical temperature for hydrogen. The uptake achieves 3.2 wt % at a rather high pressure, 12 MPa. This uptake cannot reach the target of 6.5 wt % set by the Department of Energy (DOE) of USA. However, this value complies with the theoretical estimation by Simonnyan and Johnson.[9] On the other hand, with respect to some other carbon materials reported in the literature, for example activated carbons, SWNTs and MWNTs, it is comparable or even better.[8]

When the temperature is lowered to 77 K, a pronounced improvement of hydrogen adsorption is attained. A steep increase of adsorption emerges in the range of pressure of 0−2.0

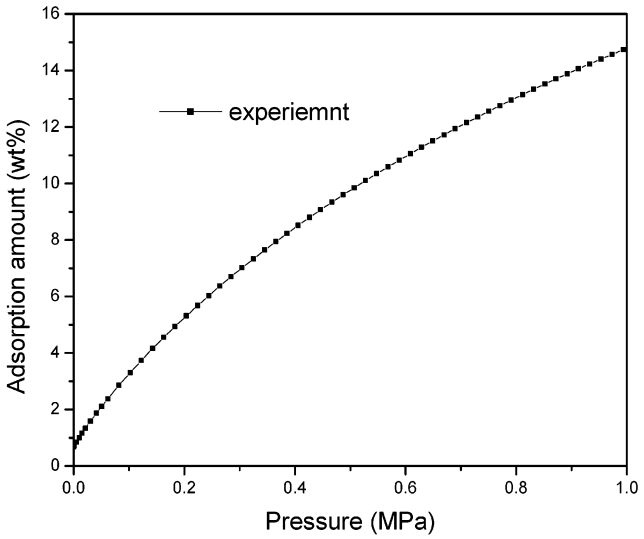

Figure 8. The experimental isotherm of methane on a-MCMBs at 298 K.

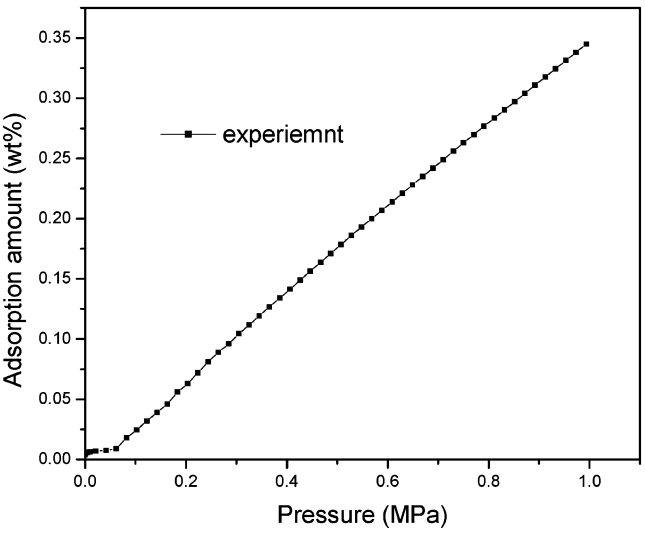

Figure 9. The experimental isotherm of hydrogen on a-MCMBs at 298 K.

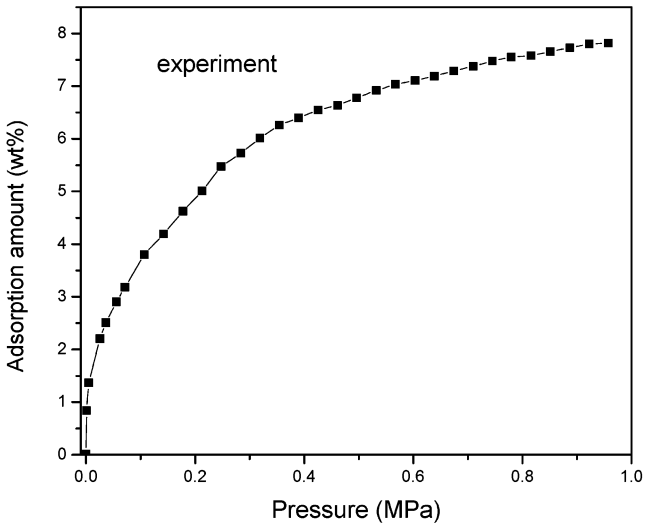

Figure 10. The experimental isotherm of hydrogen on a-MCMBs at 77 K.

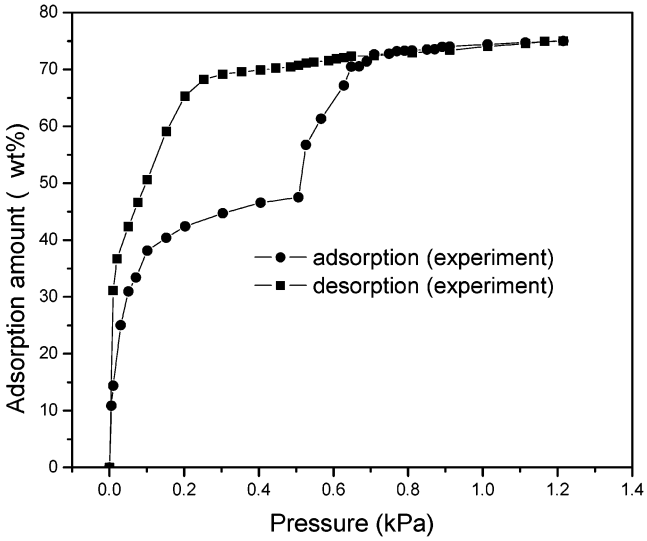

Figure 11. The experimental adsorption−desorption isotherms of methane at 77 K (● adsorption, ■ desorption).

MPa, at which the adsorption can reach about 10.25 wt %, as is shown in Figure 17. The increase of adsorption becomes flattened from 2 to 10.0 MPa, though the hydrogen adsorption amount can reach 15 wt % at 10 MPa.

As is mentioned above, capillary condensation happens for methane at 77 K and a low pressure, about 0.5 kPa. The simulated results for methane at 77 K are addressed in the next section.

Comparison between Experimental and Simulated Hysteresis Loops for Methane at 77 K. A gas−liquid transition will occur when the temperature is below the pore critical temperature, and the pore width is greater than a few times of the adsorbate molecule diameter. Such a transition appears in the adsorption isotherm as a sudden and large jump in the amount adsorbed at the capillary condensation pressure. In an idealized material with a uniform pore size, the condensation would be a sharp transition and it will have a sudden vertical jump in adsorption.[41] In a real system, this jump is often replaced by a steep increase, because a real material possesses a distribution of pore sizes.

Capillary condensation was observed for methane at 77 K in our experiment (see Figure 11). We simulated the isotherm by GCMC with PSD, which is shown along with the experimental result in Figure 18. It is found in Figure 18 that the experimental and simulated hysteresis loops coincide fairly, although the simulated capillary condensation pressure is slightly lower and the condensation density is a little higher than the experimental ones. The deviations might be caused by the assumptions introduced in our simulations.

Conclusions

It is a challenging task to develop and characterize new carbonaceous materials for adsorption storage of methane that is a major component in natural gas and hydrogen that is the cleanest energy theoretically and experimentally. We have prepared the activated mesocarbon microbeads (MCMBs) from the raw material of the filtrated residue of petroleum and carbon. The isotherm of nitrogen on the Accelerated Surface Area and Porosimetry Apparatus (ASAP 2010, Micromeritics Ins. Corp.) at 77 K, as is shown in Figure 4, provides not only the properties for the sample, e.g., the BET specific surface area of 3180m^2/g, etc., but also a basis for modeling the new material in this work.

To test the capabilities of the sample of a-MCMBs, adsorption of methane and hydrogen at 298 and 77 K is measured in the

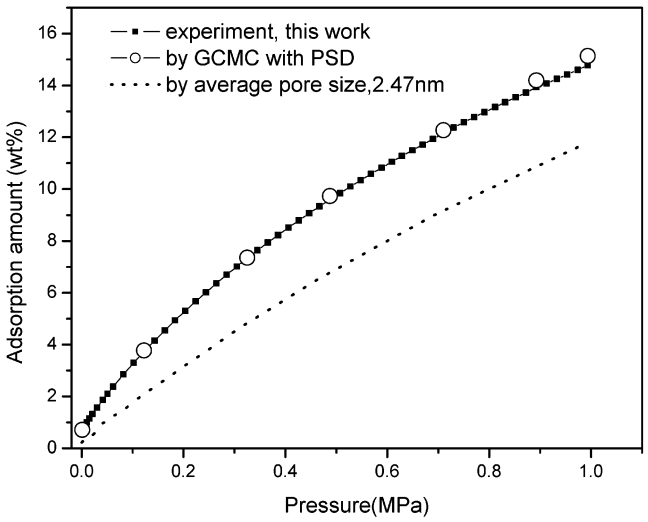

Figure 12. Comparison of simulated and experiment data of methane adsorption on a-MCMBs at 298 K (−■− experimental data (this work), −○− simulated data by PSD, • • • simulation data by the experimental average pore size, H_{av} = 2.47 nm).

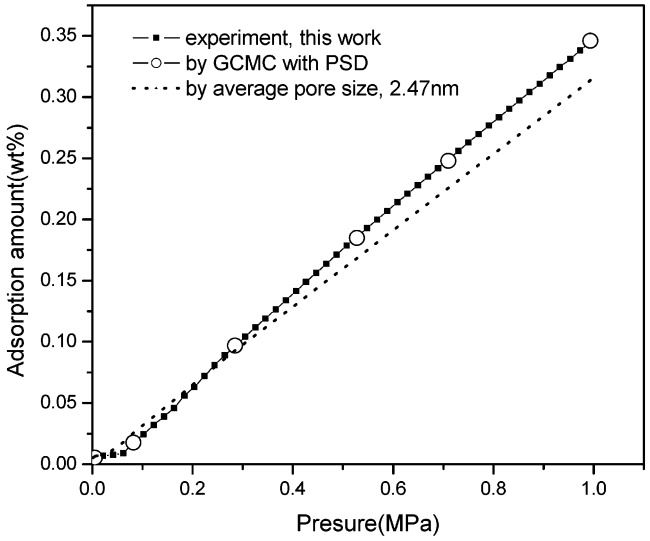

Figure 13. Comparison of simulated and experiment data of hydrogen adsorption in a-MCMBs at 298 K (−■− experimental data (this work), −○− simulation data by PSD, • • • simulation data by the experimental average pore size, H_{av} = 2.47 nm).

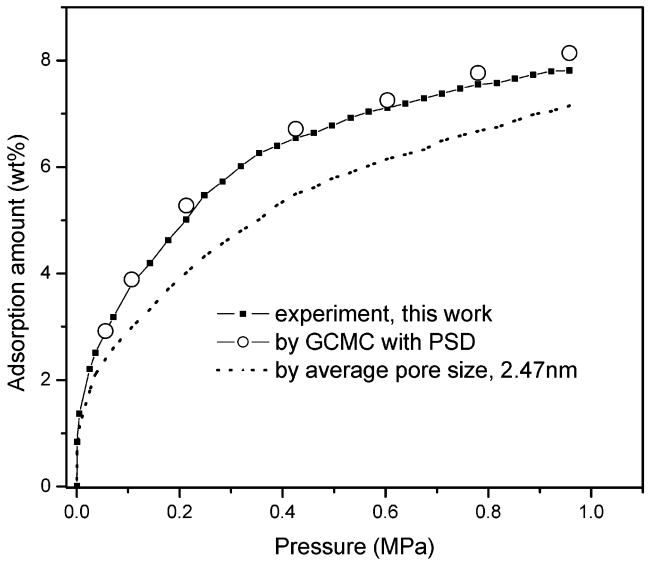

Figure 14. Comparison between experimental and simulated data of hydrogen at 77 K (−■− experimental data (this work), −○− simulation data by PSD, • • • simulated data by the experimental average pore size, H_{av} = 2.47 nm).

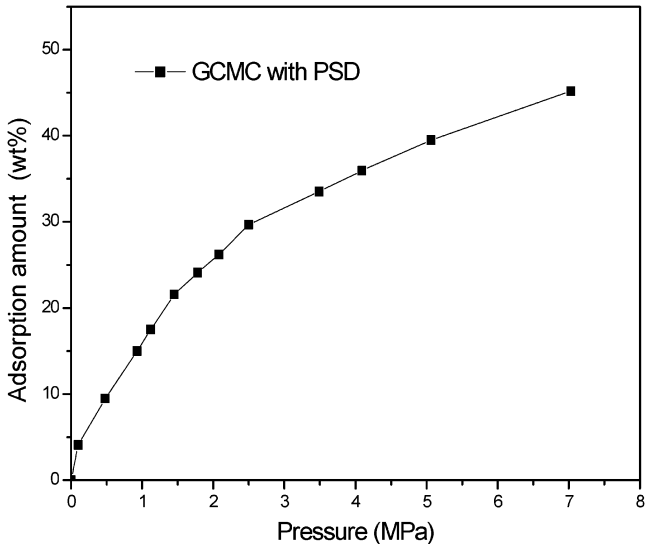

Figure 15. Methane adsorption at 298 K and high pressures on a-MCMBs predicted by GCMC and PSD.

Intelligent Gravimetric Analyzer (IGA-003, Hiden) by using the gravimetric method, as is shown in Figures 8−11. To further characterize the sample of a-MCMBs, and to predict its performances covering a wide range of pressure, a model for the material and adsorption is proposed.

In modeling of the sample of a-MCMBs, a grand canonical Monte Carlo (GCMC) method is used for the simulation of adsorption. The pores are accounted for slitlike with a pore size distribution (PSD), which is a description of the heterogeneity of the pores. The fluid−fluid and fluid−wall molecular interactions are described by the LJ and the well-known Steele's 10-4-3 potentials. The PSD obtained by the GCMC and statistical integration methods suggests that our sample is composed of micro-, meso-, and macropores, which correspond to three types of adsorption isotherms (see Figure 5). In fact, the adsorption on the sample reflects a combination of the three different behaviors.

Good agreements between the simulated and experimental isotherms for nitrogen at 77 K (see Figure 7) and isotherms for methane and hydrogen at 298 and 77 K (see Figures 12−14) are obtained. Impressively, even for the isotherms of methane at 77 K, where rather complicated hysteresis loops emerge, both the experimental and simulated results coincide fairly, as is shown in Figure 18. These observations indicate that the model proposed is a good representation of the sample of a-MCMBs, and can be furthermore used for prediction of the performances of the sample.

Predictions of the adsorption isotherms of methane and hydrogen at 298 and 77 K, up to 12 MPa are presented in Figures 15−17, respectively. It is found that the methane adsorption reaches 36 wt % at 4.0 MPa and 298 K. To our knowledge, this uptake is superior to the results reported in the literature,[15] in which the maximum uptake is 19.1 wt % on a commercial powdered activated carbon.

It is more interesting to focus on the adsorption storage of hydrogen. Hydrogen adsorption exhibits a linear increase with pressure at 298 K, as is shown in Figure 16. The uptake is 3.2 wt % at 12 MPa. This uptake does not satisfy the target of 6.5

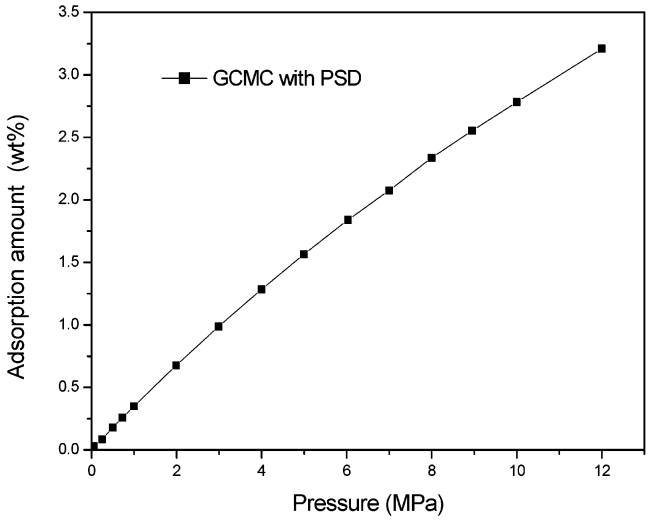

Figure 16. Hydrogen adsorption at 298 K and high pressures on a-MCMBs predicted by GCMC and PSD.

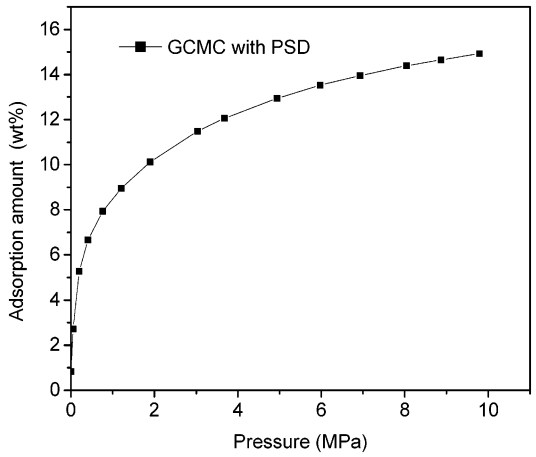

Figure 17. Hydrogen adsorption at 77 K and high pressures on a-MCMBs predicted by GCMC and PSD.

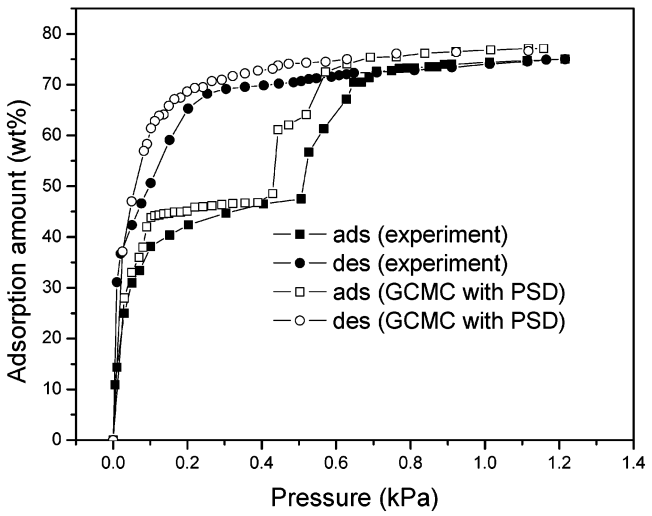

Figure 18. Comparison of experimental and simulated isotherms of methane at 77 K −■− adsorption isotherm by experiment, −●− desorption isotherm by experiment, −□− adsorption isotherm by GCMC with PSD, −○− desorption isotherm by GCMC with PSD.

wt % set by the Department of Energy (DOE) of USA. However, this value complies with the theoretical estimation by Simonnyan and Johnson.[9] On the other hand, with respect to some other carbon materials reported in the literature, for example activated carbons, SWNTs and MWNTs, it is comparable or even better.[8] At low temperature 77 K, the adsorption can reach about 10.25 wt % at 2.0 MPa and 15 wt % at 10.0 MPa, respectively, as is shown in Figure 17.

To summarize, this work presents an approach for experimental and theoretical characterization of not only the a-MCMBs but also other new adsorbents. In addition, the a-MCMBs prepared in this work seem to be an excellent candidate of adsorbents for adsorption storage of methane at ambient temperature. However, although it exhibits good capabilities for adsorption storage of hydrogen among all the current carbonaceous materials, its performances still need to be improved in terms of surface modification or other chemical doping method. This will be addressed in our future work.

Acknowledgment. This work was supported by the Key Fundamental Research Plan (No. G2000048010) and the National Natural Science Foundation of China (No. 20236010). The authors are grateful to Professor Z. L. Sun and Mr. L. H. Duan of the Liaoning University of Petroleum and Chemical Technology, Professor J. F. Chen and Mr. Z. G. Shen of the Beijing University of Chemical Technology for their help in the experimental measurements.

References and Notes

(1) Huang, M. C.; Chou, Chia-Huei; Teng, H. Pore-Size Effects on Activated-Carbon Capacities for Volatile Organic Compound Adsorption. *AIChE* **2002**, *48*, 8.

(2) Zhang, X. R.; Wang, W. C. Methane Adsorption in Single-Walled Carbon Nanotubes Arrays by Molecular Simulation and Density Functional Theory. *Fluid Phase Equilib.* **2002**, *194*−*197*, 289.

(3) Cao, D. P.; Wang, W. C.; Duan, X. Grand Canonical Monte Carlo Simulation for Determination of Optimum Parameters for Adsorption of Supercritical Methane in Pillared Layered Pores. *J. Colloid Interface Sci.* **2002**, *254*, 1.

(4) Darkrim, F. L.; Malbrunot, P.; Tartaglia, G. P. Review of Hydrogen Storage by Adsorption in Carbon Nanotubes. *Int. J. Hydrogen Energy* **2002**, *27*, 193.

(5) Wang, Q.; Johnson, J. K. Computer Simulations of Hydrogen Adsorption on Graphite Nanofibers. *J. Phys. Chem. B* **1999**, *103* (2), 277.

(6) Darkrim, F. L.; Levesque, D. High Adsorptive Property of Opened Carbon Nanotubes. *J. Phys. Chem. B* **2000**, *104*, 6773.

(7) Liu, J.; Rinzler, A. G.; Dai, H. J.; Hafner, J. H.; Bradley, R. K.; Boul, P. J.; Lu, Adrian; Iverson, T.; Shelimov, K.; Huffman, C. B.; Rodriguez-Macias, F.; Shon, Young-Seok; Lee, T. Randall; Colbert, Daniel T.; Smalley, Richard E. Fullerene Pipes. *Science* **1998**, *280*, 1253.

(8) David, P.; Piquero, T.; Metenier, K.; Pierre, Y.; Demoment, J.; Lecas-Hardit, A. Hydrogen Adsorption in Carbon Materials. The International Conference on Carbon, Sept 15−20, Beijing, China 2002.

(9) Vahan, V. Si.; Johnson, J. K. Hydrogen Storage in Carbon Nanotubes and Graphitic Nanofibers. *J. Alloys Compd.* **2002**, *330*−*332*, 659.

(10) Wang, Q.; Johnson, J. K. Computer Simulations of Hydrogen Adsorption on Graphite Nanofibers. *J. Phys. Chem. B* **1999**, *103* (2), 277.

(11) Wang, Q.; Johnson, J. K. Molecular Simulation of Hydrogen Adsorption in Single-Walled Carbon Nanaotubes and Idealized Carbon Pores. *J. Chem. Phys.* **1999**, *110*, 577.

(12) Darkrim, F. L.; Malbrunot, P.; Tartaglia, G. P. Review of hydrogen storage by adsorption in carbon nanotubes. *Int. J. Hydrogen Energy* **2002**, *27*, 193.

(13) Alcaniz-Monge, J.; Dela Casa-Lillo, M. A.; Cazorla-Amoros, D.; Linares-Solano, A. Methane Storage in Activated Carbon Fibres. *Carbon* **1997**, *35* (2), 291.

(14) Quinn, D. F.; MacDonald, J. A. Natural Gas Storage. *Carbon* **1992**, *30*, 1097.

(15) Lozano-Castello, D.; Alcaniz-Monge, J.; de la Casa-Lillo, M. A.; Cazorla-Amoros, D.; Linares-Solano, A. Advances in the Study of Methane Storage in Porous Carbonaceous Materials. *Fuel* **2002**, *81*, 1777.

(16) Lozano-Castello, D.; Cazorla-Amoros, D.; Linares-Solano, A.; Quinn, A. Activated Carbon Monoliths for Methane Storage: Influence of Binder. *Carbon* **2002**, *40*, 2817.

(17) Ishii, C.; Kaneko, K. Surface and Physical Properties of Microporous Carbon Spheres. *Prog. Org. Coatings* **1997**, *31*, 147.

(18) Ishii, C.; Matsumura, Y.; Kaneko, K. Ferromagnetic Behavior of Superhigh Surface-Area Carbon. *J. Phy. Chem*. **1995**, *99* (16), 5743.

(19) Yun, M. S.; Moon, S. L.; Doh, C. H.; Lee, K. H. Application of carbon to anode material for the lithium secondary battery. *Synth. Met.* **1995**, *71*(1−3), 1761.

(20) Ishii, C.; Shindo, N.; Kaneko, K. Random Magnetism of Superhigh Surface Area Carbon Having Minute Graphitic Structure. *Chem. Phy. Lett*. **1995**, *242*, 196.

(21) Kendall, T. T.; Gubbins, K. E. Modeling Structural Morphology of Microporous Carbons by Reverse Monte Carlo. *Langmuir* **2000**, *16*, 5761.

(22) Xue, R. S.; Shen, Z. M. The Activation of the Mesophase Pitch Microbeads. *Carbon Technol. (Chinese)* **2001**, *5*, 1.

(23) Xue, R. S.; Shen, Z. M. Effects of KOH/MMB Weight Ratio on Structure and Morphology of Activated Mesophase Carbon Microbeads. *Mater. Sci. Technol. (Chinese)* **2002**, *10* (4), 346.

(24) Honda, H. Mesophase Pitch and Meso-carbon Microbeads. *Mol. Cryst. Liq. Cryst.* **1983**, *94*, 97.

(25) Wang, Q.; Johnson, J. K.; Broughton, J. Q. Thermodynamic Properties and Phase Equilibrium of Fluid Hydrogen from Path Integral Simulations. *Mol. Phys.* **1996**, *89* (4), 1105.

(26) Silvera, I. F.; Goldman, V. V. The Isotropic Intermolecular Potential for H_2 and D_2 in the Solid and Gas Phases. *J. Chem. Phys.* **1978**, *69* (9), 4209.

(27) Buch, V. Path-Integral Simulations of Mixed Para-D-2 and Orito-D-2 Clusters—The Orientational Effects. *J. Chem. Phys*. **1994**, *100*, 7610.

(28) Buck, U.; Huisken, F.; Kohlhase, A.; Otten, D. State Resolved Rotational Excitation in D2+H2 Collisions. *J. Chem. Phys*. **1983**, *78*, 4439.

(29) Dondi, M. G.; Valbusa, U. Energy Dependence of the Differential Collision Cross Section for Hydrogen at Thermal Energies. *Chem. Phys. Lett*. **1972**, *17*, 137.

(30) Steele, W. A. The Physical Interaction of Gases with Crystalline Solids. *Surf. Sci.* **1973**, *36*, 317.

(31) Jiang, S.; Rhykerd, C. L.; Gubbins, K. E. Layering, Freezing Transitions, Capillary Condensation and Diffusion of Methane in Slit Carbon Pores. *Mol. Phys*. **1993**, *79* (2), 373.

(32) Zhou, J.; Wang, W. C. Adsorption and Diffusion of Supercritical Carbon Dioxide in Slit Carbon Pores. *Langmuir* **2000**, *16*, 8063.

(33) Cao, D. P.; Wang, W. C. Computer simulation of adsorption recovery of CCl_4 in activated carbon and layered pillared materials at ambient temperature. *Phys. Chem. Chem. Phys.* **2002**, *4*, 3720.

(34) Wang, Y. G.; Egashira, M.; Ishida, S.; Korai,Y.; Ochida, I. Microstructure of Mesocarbon Microbeads Prepared from Synthetic Isotropic Naphthalene Pitch in the Presence of Carbon Black. *Carbon* **1998**, *37*, 307.

(35) Korai, Y.; Wang, Y. G.; Yoon, S. H.; Ishida, S.; Mochida, I.; Nakagawa, Y.; Matsumura, Y. Effects of Carbon Black Addition on Preparation of Meso-carbon Microbeads. *Carbon* **1997**, *35* (7), 875.

(36) Cao, D. P; Wang, W. C.; Shen, Z. G.; Chen, J. F. Determination of Pore Size Distribution and Adsorption of Methane and CCl_4 on Activated Carbon by Molecular Simulation. *Carbon* **2002**, *40*, 2359.

(37) Blacher, S.; Sahouli, B.; Heinrichs, B.; Lodewyekx, P.; Pirard, R.; Pirard, J. P. Micropore Size Distributions of Activated Carbons. *Langmuir* **2000**, *16*, 6754.

(38) Heuchel, M.; Davies, G. M.; Buss, E.; Seaton, N. A. Adsorption of Carbon Dioxide and Methane and Their Mixtures on an Activated Carbon: Simulation and Experiment. *Langmuir* **1999**, *15*, 8695.

(39) El-Merraoui, M.; Aoshima, M.; Kaneko, K. "Micropore Size Distribution of Activated Carbon Fiber Using the Density Functional Theory and Other Methods. *Langmuir* **2000**, *16*, 4300.

(40) Sangwichien, C.; Aranovich, G. L.; Donohue, M. D. Density Functional Theory Predictions of Adsorption Isotherms with Hysteresis Loops. *Colloids Surf. A*: *Physicochem. Eng. Aspects* **2002**, *206*, 313.

(41) Gelb, D.; Gubbins, K. E.; Radhakrishnan, R.; Sliwinska-Bartkowiak, M. Phase Separation in Confined Systems. *Rep. Prog. Phys.* **1999**, *62*, 1573.